



Cite this: *RSC Adv.*, 2017, 7, 54203

# Application of functionalized ether in lithium ion batteries

Fang Hu<sup>ab</sup> and Taeseup Song<sup>ID</sup>\*<sup>a</sup>

Ethers can be typically categorized as chain ethers, aromatic ethers and crown ethers. Compounds with ether groups play an important role in chemistry, biology and functional materials. Ether acts as an anesthetic in medicine, and crown ethers are used to construct mechanically interlocked molecules. Lithium ion batteries are becoming more and more important in our modern life as our mobile devices such as smart phones and laptop computers need power supplies. In recent years, the ethers have been explored to improve the electrochemical properties of lithium ion batteries. Depending on the function of the ether groups, they are widely used as electrolytes, additives, binders, separators or anodes. In this paper, we review the progress that has been made in the use of functionalized ethers in lithium ion batteries and the synthesis strategies for them, and present the future research direction of functionalized ethers in lithium ion batteries.

Received 7th October 2017  
 Accepted 11th November 2017

DOI: 10.1039/c7ra11023e

[rsc.li/rsc-advances](http://rsc.li/rsc-advances)

## Introduction

Ethers can be typically categorized as chain ethers, aromatic ethers and crown ethers. As one example of chain ether groups, alkyl ethers have been widely used as detergents, dispersants, dyeing aids and antistatic agents.<sup>1,2</sup> Ether acts as an anesthetic in medicine. Aromatic ethers have a good solid structure, and can be used to improve a material's thermal properties and structural stability. Aromatic ether-containing epoxy resin is a type of thermosetting polymer composite with corrosion resistance and high strength.<sup>3,4</sup> It plays an important role in

industrial fields such as transistors, microchips and semi-conductors. Crown ethers are used to construct mechanically interlocked molecules.<sup>5-7</sup> Mechanically interlocked molecules are classified mainly as rotaxanes and catenanes. With the functionalization of mechanically interlocked molecules, crown ether-based molecular motor, molecular muscle and molecular shuttle have gradually been constructed. Moreover, some functionalized crown ethers, such as crown ether-based photochromic materials<sup>8</sup> and aggregation-induced fluorescence enhancement (AIE) materials,<sup>9</sup> have potential applications in many fields such as molecular switches and self-assembly systems.

Lithium ion batteries (LIBs) are becoming a more and more important part of our modern life. Many devices such as mobile televisions, smart phones and pocket computers need power sources, and the lithium ion battery is an excellent candidate for

<sup>a</sup>Department of Energy Engineering, Hanyang University, Seoul 133791, Korea. E-mail: [tssong@hanyang.ac.kr](mailto:tssong@hanyang.ac.kr)

<sup>b</sup>Faculty of Materials Science and Chemical Engineering, Ningbo University, Ningbo 315211, PR China



*Fang Hu received her Ph.D. degree from the College of Chemistry at CCNU, PR China in 2015. She joined Hanyang University as a post-doctor in 2017. She became an assistant professor at Ningbo University from 2015. Her research interests focus on lithium ion batteries, supercapacitors and electrocatalysis.*




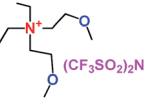


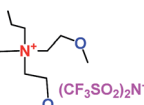
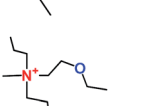
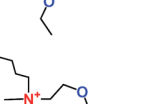
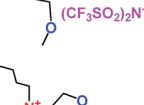
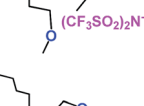


*Taeseup Song received his Ph.D. degree from the Department of Materials Science and Engineering at Hanyang University, Korea in 2012. He is currently an assistant professor at Hanyang University. His research interest is mainly focused on the synthesis of nanostructured materials for energy device applications.*





**Table 1** Representative structures, electrochemical windows, viscosity ( $\eta$ ) and conductivity ( $\sigma$ ) of quaternary ammonium ionic liquids with two ether groups at 25 °C (ref. 26)

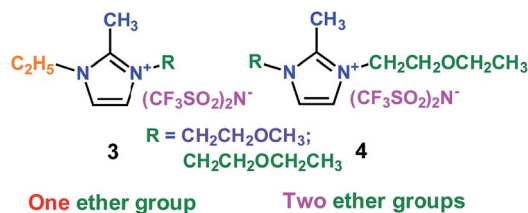
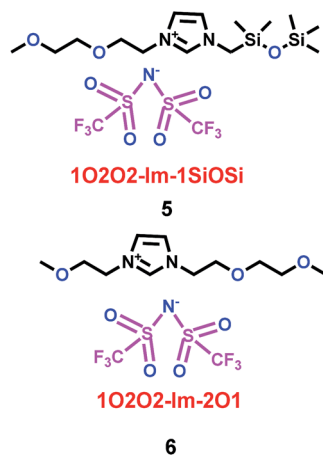
Structure	Cathodic limiting potential $V$ vs. $\text{Li}/\text{Li}^+$	Anodic limiting potential $V$ vs. $\text{Li}/\text{Li}^+$	Electrochemical window $V$	$\eta$ (mPa s)	$\sigma$ ( $\text{mS cm}^{-1}$ )
	0.2	5.3	5.1	203.1	0.83
	0.2	5.2	5.0	182.3	0.78
	0.3	5.3	5.0	165.2	0.74
	0.2	5.2	5.0	230.8	0.70
	0.3	5.3	5.0	212.6	0.66
	0.2	5.3	5.1	243.1	0.60
	0.3	5.3	5.0	238.8	0.58
	0.3	5.3	5.0	231.2	0.54
	0.2	5.2	5.0	263.6	0.48
	0.2	5.3	5.0	259.3	0.42
	0.1	5.2	5.1	248.1	0.46

viscosity and higher conductivity, which could be due to the lower melting points and higher thermal decomposition temperatures with the presence of the ether group and FSI anion. More importantly, the PZ2o2-2-FSI with more alkyl groups possessed

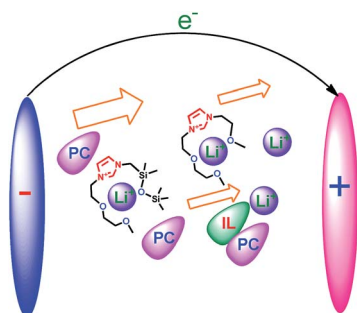
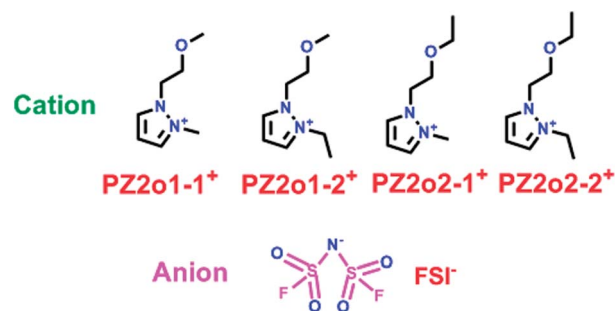
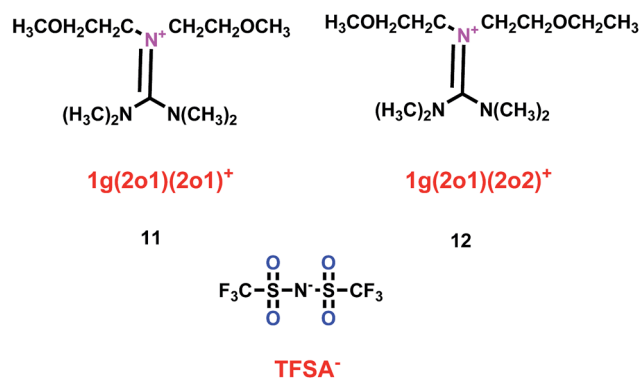
the lowest viscosity, while the PZ2o1-2-FSI had the highest conductivity because of the presence of the methoxy group.

As well as some normal cation ionic liquids, guanidinium cation ionic liquids can act as electrolytes for lithium ion



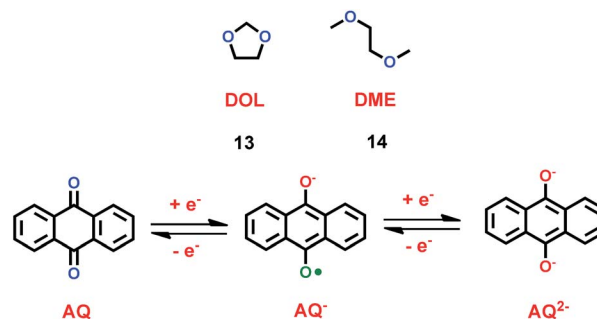
Scheme 3 The structures of trialkylimidazolium ionic liquids.<sup>27</sup>Scheme 4 The structures of imidazolium ionic liquids.<sup>28</sup>

batteries, Yang's group found that ether-functionalized guanidinium cation ionic liquids could also be used as electrolytes (**11** and **12**) (Scheme 7).<sup>30</sup> Because of the importance of viscosity for the lithium ion battery, the viscosities of 1g(2o1)(2o1)-TFSA (**11**) and 1g(2o1)(2o2)-TFSA (**12**) were checked and found to have the values of 60.2 and 58.8 mPa s respectively at 25 °C. When these ether-functionalized ionic liquids based on guanidinium cation were used as electrolytes in Li/LiFePO<sub>4</sub> batteries, these batteries showed electrochemical stability and good cycling properties at the current rate of 0.2 C owing to the formation of a passivation layer. Moreover, without any additive, obvious lithium plating and stripping could be found on the Ni electrode when the ether-functionalized guanidinium cation ionic liquids were used as electrolytes for the lithium ion battery,

Scheme 5 The electrochemical behaviors of **5** and **6** as electrolytes for LIBs.<sup>28</sup>Scheme 6 The structures of pyrazolium ionic liquids.<sup>29</sup>Scheme 7 The structures of guanidinium cation ionic liquids.<sup>30</sup>

which was attributed to the present of solid–electrolyte interface (SEI) film.

As liquid electrolytes, ether-based cation ionic liquids with low viscosity are usually used in lithium ion batteries. Organic solvents with ether groups are also good in lithium ion batteries. Chen and co-workers found that anthraquinone (AQ) was a good candidate for the cathode material in lithium ion batteries, as shown in Scheme 8.<sup>31</sup> For most of the inorganic compounds that are used as cathode material in lithium ion batteries, cation ionic liquids are good options. But for organic cathode compounds, some simple electrolytes such as 1,3-dioxetane (DOL) (**13**) and dimethyl ether (DME) (**14**) are useful. With LiNO<sub>3</sub> additive and ether-based electrolyte, a lithium ion battery with anthraquinone as cathode showed good cycling

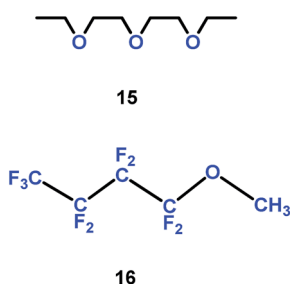
Scheme 8 The structures of organic solvents with ether groups.<sup>31</sup>

and rate performance. Compared with the carbonate-based electrolyte, the discharge capacity and retention capacity of this lithium ion battery can reach  $174 \text{ mA h g}^{-1}$  and 84.9% after 100 cycles at 0.2 C. Furthermore, the lithium ion battery with ether-based electrolyte delivered high discharge capacities at both low and high rates. With  $\text{LiNO}_3$  additive, the ether-based electrolyte can form a protective film on the surface of the anode to prevent the SEI forming. Compared with other electrolytes, ether-based electrolytes effectively decrease the solubility of anthraquinone, which is good for lithium ion transportation. This means the introduction of an ether group can improve the high cycling and rate performance of the lithium ion battery.

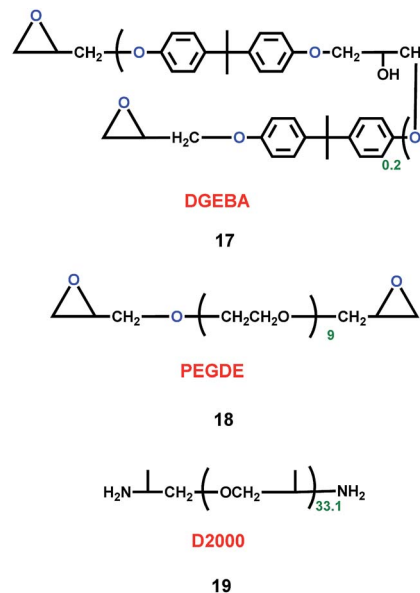
For cation ionic liquids, the presence of an ether group can reduce the viscosity for use in lithium ion batteries, increase the electrochemical stability and improve the cycling properties. In contrast, the organic solvents with ether groups improve the cycling and rate performance of the lithium ion battery by decreasing the solubility of the cathode.

Organic solvent alkyl ethers could be used as electrolytes. Yang and co-authors introduced the trifluoromethyl group into organic solvent alkyl ethers, and found that a mixture of diethylene glycol diethylether (15) and non-flammable methyl-nonafluorobutyl ether (16) could be employed as electrolyte for lithium ion batteries (Scheme 9).<sup>32</sup> Compared with the conventional electrolytes, these electrolytes gave better rate, cycling and low-temperature performances for graphite/ $\text{LiFePO}_4$  cells.

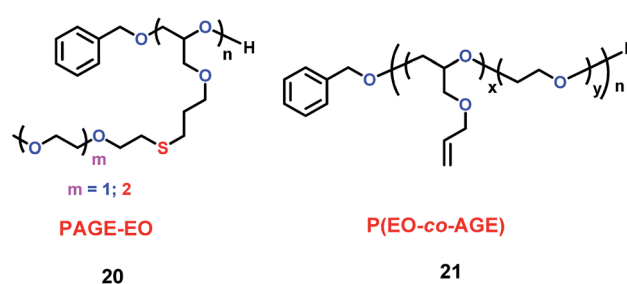
As well as cation ionic liquids and organic solvent alkyl ethers, polymers could also act as electrolytes for lithium ion batteries. Teng's group synthesized three polymers (17, 18 and 19) (Scheme 10).<sup>33</sup> By mixing the three polymers, the P(EO-co-PO) polymeric framework of the electrolyte was gained. The P(EO-co-PO) polymeric framework exhibited high ionic conductivity. In particular, the high solvent-coordinating ability of ether groups in the P(EO-co-PO) polymeric framework created free volume for ion motion, which facilitated the transport of solvent-solvated  $\text{Li}^+$  ions through the segmental movement of polymer chains. When it was used in the graphite|GPE| $\text{LiFePO}_4$  battery, the P(EO-co-PO) polymeric framework had high ionic conductivity and lithium transference number. Also, the P(EO-co-PO) polymeric framework exhibited smaller interfacial resistance against lithium metal. Compared with the carbonate solvent, the P(EO-co-PO) polymeric framework stabilized the



Scheme 9 The structures of organic solvent alkyl ethers.<sup>32</sup>



Scheme 10 The structures of polymers.<sup>33</sup>



Scheme 11 The structure of poly(allyl glycidyl ether).<sup>34</sup>

solvent and suppressed the formation of thick SEI layers that hinder interfacial ion transport.

Hawker's group found that the poly(allyl glycidyl ether) (PAGE) platform could be used as electrolyte (Scheme 11).<sup>34</sup> In the structure of these electrolytes (20 and 21), the allyl ether could prevent the formation of nonconducting crystalline regions, which are bad for ion conduction. Additionally, the introduction of ethylene oxide oligomer could increase the conductivity. They found that these electrolytes have conductivities near  $10^{-4} \text{ S cm}^{-1}$  at room temperature. The properties of 21 are summarized in Tables 2 and 3.

## Additive

In the lithium manganite/carbon (LMO-GR) cell, lithium manganite's activity determined the performance of the battery. Dissolved Mn ions from the positive electrode (lithium manganite) migrated to and were deposited on the negative electrode (carbon), which degraded the cell's performance for lithium ion batteries (LIBs). In order to prevent dissolved Mn ions from reaching the negative electrode, Levi's group synthesized two crown ether-based polymers, poly(undecylenyl





Table 2 P(EO-co-AGE) characterization and properties<sup>34</sup>

Molar feed ratio [EO]/[AGE]	Polymer% EO (wt)	$M_w$ (kg mol <sup>-1</sup> ) by NMR	$M_n$ (kg mol <sup>-1</sup> ) by GPC	PDI	$T_g$ (°C)	$X_c$ (%)
PEO	100	n. a.	33.7	1.07	n. a.	86
7.5	77	39.4	29.5	1.12	-69	32
5	69	16.9	14.3	1.21	-70	23
4	61	14.7	15.8	1.13	-71	15
3	56	6.5	7.9	1.13	-69	0
1	32	27.5	17.3	1.11	-73	0

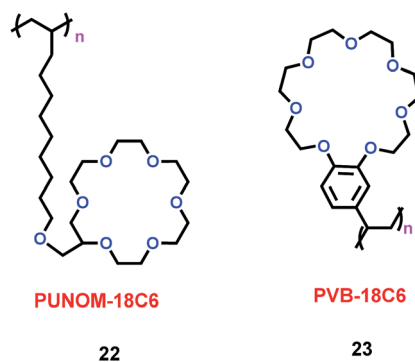
Table 3 Glass transition temperature and Vogel–Tamman–Fulcher (VTF) parameters for polymer electrolytes<sup>34</sup>

[O]/[Li]	$r = \frac{[Li]}{[O]}$	$w_{LITFSI}$	$T_g^a$ (°C)	$E_a$ (kJ mol <sup>-1</sup> )	$\sigma_0$ (S cm <sup>-1</sup> )
[Li] = 0	0	0.00	-78.0	5.96	$6.24 \times 10^{-7}$
90	0.01	0.05	-75.8	9.02	$5.11 \times 10^{-3}$
52	0.02	0.09	-74.0	9.58	$1.97 \times 10^{-2}$
32	0.03	0.13	-72.0	9.82	$4.54 \times 10^{-2}$
26	0.04	0.16	-67.5	10.4	$1.58 \times 10^{-1}$
16	0.06	0.24	-58.4	9.8	$2.33 \times 10^{-1}$
10	0.10	0.33	-49.3	9.47	$2.79 \times 10^{-1}$

<sup>a</sup> Measured by differential scanning calorimetry (DSC).  $T_0$  set to  $T_g - 50$  K in VTF fits to conductivity data.

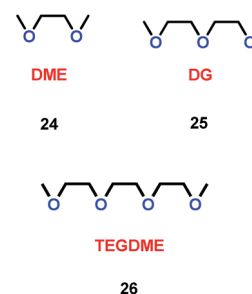
oxymethyl-18-crown-6) (PUNOM-18C6) (22) and poly(vinylbenzo-18-crown-6) (PVB-18C6) (23) (Scheme 12).<sup>35</sup> The PVB-18C6 polymer could trap Mn ions, which meant that the amount of manganese deposited at the negative electrode would be correspondingly reduced. Concomitantly, a 26% improvement in capacity was gained after 100 cycles of the LMO-GR. For PVB-18C6, the macrocycle and the polymer backbone were linked by the benzene ring, and the rigid link played a determining role for the Mn ion trapping ability. For PUNOM-18C6, the flexible link between the macrocycle and the polymer led to no trapping of Mn ions. Thus PVB-18C6 was better than PUNOM-18C6 as an additive for Li-ion batteries.

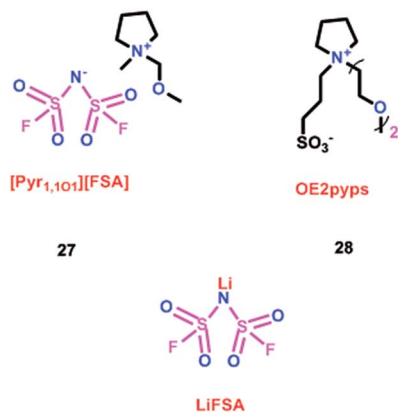
As well as crown ethers, alkyl ethers could also be used as additives for Li-ion batteries. By changing the ratio of ether/alkyl, Xie and co-workers synthesized three different ethers, 1,2-dimethoxyethane (DME) (24), diethylene glycol dimethyl ether

Scheme 12 The structures of crown ethers-based polymers.<sup>35</sup>

(DG) (25) and triethylene glycol dimethyl ether (TEGDME) (26) (Scheme 13).<sup>36</sup> With the presence of DME, the cell was faster to reach the stable state than with DG and TEGDME. The SEI film in DME was stable at the beginning of cycling. Moreover, the electrolytes containing DG and TEGDME had a higher resistance when the lithium ions migrated through the SEI film on the lithium electrode. The TEGDME-based electrolyte was more active for SEI film formation. This means that different ratios of the ether/alkyl moieties had a great impact on SEI formation, and determined the performance of the lithium ion battery.

As we all know, ionic liquids (ILs) could be used as electrolyte as well as additive. Yoshizawa-Fujita and co-workers synthesized one ionic liquid containing a zwitterion named 3-(1-(2-(2-methoxyethoxy)ethyl)pyrrolidin-1-ium-1-yl)propane-1-sulfonate (OE2pyps) (28) (Scheme 14).<sup>37</sup> For the research, *N*-methyl-*N*-methoxymethylpyrrolidinium bis(fluorosulfonyl)amide ([Py<sub>1,101</sub>][FSA]) (27) and lithium bis(fluorosulfonyl)amide (LiFSA) were used as electrolytes. When the OE2pyps was used as the additive for the lithium ion battery, the electrolyte with [Py<sub>1,101</sub>][FSA]/LiFSA had a higher viscosity and lower ionic conductivity and lithium transference number. The interactions between the sulfonate groups of OE2pyps (28) and lithium ions might have a great impact on the viscosity and ionic conductivity changes. Within the cut-off voltage range of 3.0–4.3 V, the cell had better discharge capacities during the charge/discharge tests with increasing OE2pyps content. Moreover, the cycle stability became better with the addition of OE2pyps. By adding OE2pyps into the electrolytes, the interface resistance between the electrolyte and cathode was suppressed. Therefore, using this zwitterion with its long ether group as additive for Li-ion batteries could improve their charge/discharge stability. The diffusion coefficients and lithium transference numbers are summarized in Table 4.

Scheme 13 The structures of alkyl ethers.<sup>36</sup>

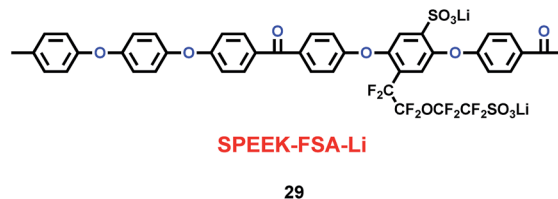
Scheme 14 The structures of ionic liquids.<sup>37</sup>

## Binder

Xue and co-workers synthesized a sulfonated poly(ether-etherketone) with pendant lithiated fluorinated sulfonic groups (SPEEK-FSA-Li) (29) (Scheme 15), and found it was a good candidate as ionic conductivity binder.<sup>38</sup> Compared with the binder PVDF, it had stronger adhesion and better stability. With the charge delocalization over the sulfonic chain, SPEEK-FSA-Li acted as binder with larger ionic conductivity and Li<sup>+</sup> ion diffusion. When the SPEEK-FSA-Li binder was mixed into the electrode, the electrode exhibited smaller resistances at the solid-electrolyte interface (SEI) and lithium ion transport, which was good for lithium ion intercalation and de-intercalation. This means that the electrode had low charge plateau potential and high discharge plateau potential. The resistance values are summarized in Table 5.

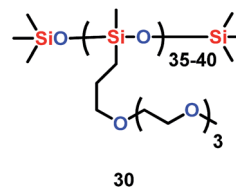
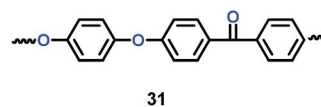
## Separator

Seidel *et al.* found that ether-modified polysiloxanes (PSx-PEO3) (30) could act as active separators for the lithium ion battery when they were blended within a poly(vinylidene fluoride-*co*-hexafluoropropylene) (PVDF-HFP) matrix (Scheme 16). Moreover, when 20 wt% of PSx-PEO3 was added into the PVDF-

Scheme 15 The structure of SPEEK-FSA-Li.<sup>38</sup>Table 5 Resistance values obtained from fitting impedance spectra<sup>38</sup>

Structure	$R_s/\Omega \text{ cm}^{-2}$	$R_f/\Omega \text{ cm}^{-2}$	$R_{ct}/\Omega \text{ cm}^{-2}$
	2.13	43.76	147.70
	1.71	8.60	88.58

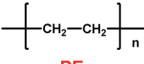
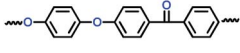
HFP matrix, the membrane system showed better ionic conductivity and cycling results than the pure PVDF-HFP system.<sup>39</sup>

Scheme 16 The structure of ether-modified polysiloxanes.<sup>39</sup>Scheme 17 The structure of PEEK.<sup>40</sup>Table 4 Diffusion coefficients and lithium transference numbers for [Pyr<sub>1,101</sub>][FSA]/LiFSA, [Pyr<sub>1,101</sub>][FSA]/LiFSA/OE2pyps (5 wt%), and [Pyr<sub>1,101</sub>][FSA]/LiFSA/OE2pyps (10 wt%) at 40 °C (ref. 37)

Structure	$D_H/m^2 \text{ s}^{-1}$	$D_F/m^2 \text{ s}^{-1}$	$D_{Li}/m^2 \text{ s}^{-1}$	$t_{Li^+}$
	$5.75 \times 10^{-11}$	$5.72 \times 10^{-11}$	$4.54 \times 10^{-11}$	0.41
	$4.00 \times 10^{-11}$	$4.71 \times 10^{-11}$	$1.31 \times 10^{-11}$	0.22
	$3.60 \times 10^{-11}$	$4.24 \times 10^{-11}$	$5.67 \times 10^{-12}$	0.12



Table 6 Physical properties of PEEK membranes and PE separators<sup>40</sup>

Structure	Thickness ( $\mu\text{m}$ )	Porosity [%]	Electrolyte contact angle [deg]	Electrolyte uptake [%]	Ion conductivity [ $\text{S cm}^{-1}$ , 25 °C]
 PE	20	40	53	111	$6.65 \times 10^{-4}$
 PEEK	30	78	29	251	$10.64 \times 10^{-4}$

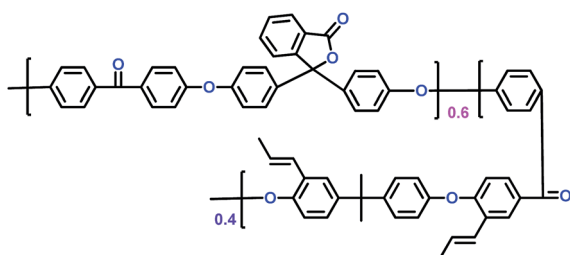
Li's group have reported a porous poly(ether-ether-ketone) (PEEK) (31) material could be used as separator in lithium ion batteries with high thermal stability and superior rate capability (Scheme 17).<sup>40</sup> Compared with the commercial polyethylene (PE) separator, the electrolyte uptake could reach 251% when the porous PEEK membrane was used, which means that it showed excellent electrolyte wettability. More importantly, the discharge capacity could reach  $124.1 \text{ mA h g}^{-1}$  with the PEEK membrane acting as separator in the lithium-ion battery, which means that it showed outstanding rate performance. The physical properties of PEEK membranes and PE separators are summarized in Table 6.

Kim's group have reported a kind of copolymer based on poly(arylene ether ketone) (PAEK) and poly(lactic acid) (PLA) structures (32) (Scheme 18). When various concentrations of PLA were added into the PAEK, the pore size and porosity of the copolymers were different.<sup>41</sup> Compared with commercial poly(propylene) (PP) separator, the copolymers based on PAEK and



PAEK-PLA

32

Scheme 18 The structure of PAEK-PLA.<sup>41</sup>

P-PAEK

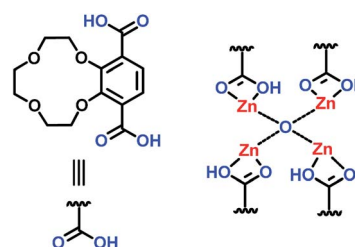
33

Scheme 19 The structure of P-PAEK.<sup>42</sup>

PLA had better liquid electrolyte uptake, excellent thermal and mechanical stability, and higher lithium ion conductivity, which means the copolymers were a good candidate for separator. Based on the PAEK structure, Liu and co-workers found that phenolphthalein and allyl groups-modified PAEK (P-PAEK) (33) could also be used as an excellent composite separator for the lithium ion battery when it was mixed with PVDF (Scheme 19). It had high porosity, uniform pore distribution and low thermal shrinkage.<sup>42</sup>

## Anode

A microporous Zn-based metal-organic framework (MOF) containing 12-crown-4 units (Zn-MOF-Crown) (34) was constructed by Zhao's group (Scheme 20).<sup>43</sup> This material could be used as the anode material in the lithium ion battery, with a charge capacity of  $273 \text{ mA h g}^{-1}$ . More importantly, it retained 88% of its capacity after 500 cycles. During charge and discharge, the MOF structure integrity never was damaged because of the interaction between the  $\text{Li}^+$  ions and crown ether. Interestingly, when the Zn-MOF-Crown complexed with  $\text{Li}^+$  ions and  $\text{Li}^+@Zn\text{-MOF-Crown}$  was formed, it had better electrochemical performance, with a charge capacity of  $348 \text{ mA h g}^{-1}$  and long-term cycling ability. This means the introduction of crown ether could improve the performance in green energy systems. The properties of different MOFs or MOF-derived materials for LIBs are summarized in Table 7. Compared with other MOF-derived materials, crown ether-based MOFs had longer-term cycling ability with high charge capacity.



Crown ether


Zn-MOF-Crown

34

Scheme 20 The structure of Zn-MOF-Crown.<sup>43</sup>



Table 7 MOF or MOF-derived materials for LIBs<sup>43</sup>

Structure	Charge capacity/discharge capacity (mA h g <sup>-1</sup> )	Reversible capacity (mA h g <sup>-1</sup> )	Cycle number
 Zn-MOF-Crown	273/405	239	500
[Fe <sup>III</sup> (OH) <sub>0.8</sub> F <sub>0.2</sub> (O <sub>2</sub> CC <sub>6</sub> H <sub>4</sub> CO <sub>2</sub> )]·H <sub>2</sub> O, MIL-53	70/80	71	50
MIL-177	110/425	—	2
Zn <sub>3</sub> (HCOO) <sub>6</sub>	693/1344	560	30
Co <sub>3</sub> (HCOO) <sub>6</sub>	870/1720	390	60
Zn <sub>1.5</sub> Co <sub>1.5</sub> (HCOO) <sub>6</sub>	930/1570	450	60
Mn-LCP	610/1870	390	5
Co <sub>2</sub> (OH) <sub>2</sub> BDC	1005/1385	650	50

## Conclusions

In conclusion, ether-functionalized lithium ion batteries have been reported widely. According to the functionalization of ether groups, ethers are used mainly as electrolyte, additive, binder, separator or anode in lithium ion batteries. When functionalized cation ionic liquids were used as electrolyte, ether-based ionic liquids had better properties for LIBs, but it was very difficult to gain pure ionic liquids. Ether-based polymers could be used as electrolyte and separator. Crown ether could be utilized to construct novel additives and anodes. Compared with cation ionic liquids and polymers, crown ether was easier to synthesize, and crown ether-based metal-organic frameworks (MOFs) had better charge capacity with excellent cycling performance. Moreover, by changing the cavity size of the crown ether, it could be complexed with different metal ions such as sodium and magnesium. This means that the electrochemical performance of sodium ion batteries and magnesium ion batteries could also be improved by introducing crown ether. In the future, it will be significant to find and synthesize novel crown ether-based materials, which could be utilized to construct the anode for lithium ion batteries, sodium ion batteries and magnesium ion batteries.

## Conflicts of interest

There are no conflicts to declare.

## Acknowledgements

This work was supported by Basic Science Research Program through the National Research Foundation of Korea (NRF) funded by the Ministry of Science, ICT (2016R1C1B2007299) and National Natural Science Foundation of China (21602122).

## Notes and references

1 For selected review, see: L. He, F. Lin, X. Li, H. Sui and Z. Xu, *Chem. Soc. Rev.*, 2015, **44**, 5446–5494.

- For selected reviews, see: A. Karci, *Chemosphere*, 2014, **99**, 1–18.
- X. Gong, H. Kang, Y. Liu and S. Wu, *RSC Adv.*, 2015, **5**, 40269–40282.
- F. Liu, Z. Wang, D. Liu and J. Li, *Polym. Int.*, 2009, **58**, 912–918.
- For selected reviews, see: Z. Liu, S. Nalluri and J. F. Stoddart, *Chem. Soc. Rev.*, 2017, **46**, 2459–2478.
- G. Bo, G. Dolphijn, C. McTernan and C. Leigh, *J. Am. Chem. Soc.*, 2017, **139**, 8455–8457.
- W. Deng, A. Flood, J. F. Stoddart and W. Goddard, *J. Am. Chem. Soc.*, 2005, **127**, 15994–15995.
- F. Hu, J. Huang, M. Cao, Z. Chen, Y. Yang, S. H. Liu and J. Yin, *Org. Biomol. Chem.*, 2014, **12**, 7712–7720.
- X. Han, M. Cao, Z. Xu, D. Wu, Z. Chen, A. Wu, S. H. Liu and J. Yin, *Org. Biomol. Chem.*, 2015, **13**, 9767–9774.
- X. Wang, W. Han, H. Chen, J. Bai, T. Tyson, X. Yu, X. Wang and X. Yang, *J. Am. Chem. Soc.*, 2011, **133**, 20692–20695.
- X. Wang, S. Singh, T. Ma, C. Lv, N. Chawla and H. Jiang, *Chem. Mater.*, 2017, **29**, 5831–5840.
- A. Mascaro, Z. Wang, P. Hovington, Y. Miyahara, A. Paoletta, V. Garipey, Z. Feng, T. Enright, C. Aiken, K. Zaghbi, K. Bevan and P. Grutter, *Nano Lett.*, 2017, **17**, 4489–4496.
- For selected reviews, see: W. Li, B. Song and A. Manthiram, *Chem. Soc. Rev.*, 2017, **46**, 3006–3059.
- For selected reviews, see: Y. Tang, Y. Zhang, W. Li, B. Ma and X. Chen, *Chem. Soc. Rev.*, 2015, **44**, 5926–5940.
- Q. Truong, M. Devaraju and I. Honma, *J. Mater. Chem. A*, 2014, **2**, 17400–17407.
- Y. Feng, H. Zhang, L. Fang, Y. Ouyang and Y. Wang, *J. Mater. Chem. A*, 2015, **3**, 15969–15976.
- For selected reviews, see: J. Xie and Q. Zhang, *J. Mater. Chem. A*, 2016, **4**, 7091–7106.
- L. Fédèle, F. Sauvage and M. Bécuwe, *J. Mater. Chem. A*, 2014, **2**, 18225–18228.
- H. Park, D. Shin, T. Song, W. Park and U. Paik, *J. Mater. Chem. A*, 2017, **5**, 6958–6965.
- For selected reviews, see: T. Song and U. Paik, *J. Mater. Chem. A*, 2016, **4**, 14–31.



- 21 O. Wijaya, P. Hartmann, R. Younesi, I. Markovits, A. Rinaldi, J. Janek and R. Yazami, *J. Mater. Chem. A*, 2015, **3**, 19061–19067.
- 22 H. Fei, Y. An, J. Feng, L. Ci and S. Xiong, *RSC Adv.*, 2016, **6**, 53560–53565.
- 23 M. Cheng, L. Li, Y. Chen, X. Guo and B. Zhong, *RSC Adv.*, 2016, **6**, 77937–77943.
- 24 M. Xie, J. Wang, X. Wang, M. Yin, C. Wang, D. Chao and X. Liu, *Macromol. Res.*, 2016, **24**, 965–972.
- 25 For selected reviews, see: U. Farooqui, A. Ahmad and N. Hamid, *Renewable Sustainable Energy Rev.*, 2017, **77**, 1114–1129.
- 26 Y. Jin, J. Zhang, J. Song, Z. Zhang, S. Fang, L. Yang and S. Hirano, *J. Power Sources*, 2014, **254**, 137–147.
- 27 Y. Jin, S. Fang, M. Chai, L. Yang, K. Tachibana and S. Hirano, *J. Power Sources*, 2013, **226**, 210–218.
- 28 S. Chavan, A. Tiwari, T. Nagaiah and D. Mandal, *Phys. Chem. Chem. Phys.*, 2016, **18**, 16116–16126.
- 29 G. Wang, S. Shen, S. Fang, D. Luo, L. Yang and S. Hirano, *RSC Adv.*, 2016, **6**, 71489–71495.
- 30 Y. Jin, S. Fang, L. Yang, S. Hirano and K. Tachibana, *J. Power Sources*, 2011, **196**, 10658–10666.
- 31 K. Zhang, C. Guo, Q. Zhao, Z. Niu and J. Chen, *Adv. Sci.*, 2015, **2**, 1500018.
- 32 S. Fang, G. Wang, L. Qu, D. Luo, L. Yang and S. Hirano, *J. Mater. Chem. A*, 2015, **3**, 21159–21166.
- 33 L. Huang, Y. Shih, S. Wang, P. Kuo and H. Teng, *J. Mater. Chem. A*, 2014, **2**, 10492–10501.
- 34 K. Barteau, M. Wolffs, N. Lynd, G. Fredrickson, E. Kramer and C. Hawker, *Macromolecules*, 2013, **46**, 8988–8994.
- 35 B. Ziv, N. Levy, V. Borgel, Z. Li, M. Levi, D. Aurbach, A. Pauric, G. Goward, T. Fuller, M. Balogh and I. Halalay, *J. Electrochem. Soc.*, 2014, **161**, 1213–1217.
- 36 S. Xiong, Y. Diao, X. Dong, Y. Chen and K. Xie, *J. Electrochem. Soc.*, 2014, **719**, 122–126.
- 37 S. Horiuchi, H. Zhu, M. Forsyth, Y. Takeoka, M. Rikukawa and M. Yoshizawa-Fujita, *Electrochim. Acta*, 2017, **241**, 272–280.
- 38 Z. Wei, L. Xue, F. Nie, J. Sheng, Q. Shi and X. Zhao, *J. Power Sources*, 2014, **256**, 28–31.
- 39 S. Seidel, S. Vettikuzha and H. Wiemhofe, *Chem. Commun.*, 2015, **51**, 12048–12051.
- 40 D. Li, D. Shi, K. Feng, X. Li and H. Zhang, *J. Membr. Sci.*, 2017, **530**, 125–131.
- 41 A. Mong and D. Kim, *J. Power Sources*, 2016, **304**, 301–310.
- 42 M. Xie, M. Yin, G. Nie, J. Wang, C. Wang, D. Chao and X. Liu, *Polymer Chem.*, 2016, **54**, 2714–2721.
- 43 L. Bai, B. Tu, Y. Qi, Q. Gao, Z. Liu, D. Liu, L. Zhao, Q. Li and Y. Zhao, *Chem. Commun.*, 2016, **52**, 3003–3006.

